Electronic Supplementary Material (ESI) for CrystEngComm.

Electronic Supplementary Information for:

How similar are amorphous calcium carbonate and calcium phosphate? A comparative study of amorphous phases formation conditions

I. Buljan Meić[1], J. Kontrec[1], D. Domazet Jurašin[2], A. Selmani[2], B. Njegić Džakula[1], N. Maltar-Strmečki[2], D. M. Lyons[3], M. Plodinec[4], M. Čeh[5], A. Gajović[4], M. Dutour Sikirić[2*], D. Kralj[1*]

[1]Division of Materials Chemistry, Ruđer Bošković Institute, Bijenička c. 54, 10 000 Zagreb, Croatia
[2]Division of Physical Chemistry, Ruđer Bošković Institute, Bijenička c. 54, 10 000 Zagreb, Croatia
[3]Center for Marine Research, Ruđer Bošković Institute, Giordano Paliaga 5, 52210 Rovinj, Croatia
[4]Division of Materials Physics, Ruđer Bošković Institute, Bijenička c. 54, 10 000 Zagreb, Croatia
[5]Department of Nanostructured Materials, Jožef Stefan Institute, Jamova 39, 1000 Ljubljana, Slovenia

* Corresponding authors:

Damir Kralj
Division of Materials Chemistry
Ruđer Bošković Institute
Bijenička cesta 54, 10 000 Zagreb, Croatia
Phone: + 385 1 468 0207
Fax: + 385 1 468 0098
E-mail: kralj@irb.hr

Maja Dutour Sikirić
Division of Physical Chemistry
Ruđer Bošković Institute
Bijenička cesta 54, 10 000 Zagreb, Croatia
Phone: + 385 1 456 0941
Fax: + 385 1 468 0245
E-mail: sikiric@irb.hr

Content of listed materials

SI 1 Electron paramagnetic resonance spectroscopy

EPR spectroscopy is spectroscopic technique which consists of the resonant absorption of microwaves by unpaired electrons tuned by external magnetic field. The molecules with unpaired electron, so called free radicals can originate from transition-group ions, ferromagnetic participates, radiation-induced defect centers etc.[1] Generally, for analysis of the EPR spectra of paramagnetic species detected in calcium phosphate materials, EPR parameters g, A, D, E are used. The g tensor is a measure of coupling between the unpaired electron's spin angular momentum (S) and the orbital angular momentum (L) of paramagnetic ions such as Mn^{2+}. The g tensor is affected by the host lattice in which paramagnetic ion is incorporated. In the case of radiation induced paramagnetic molecules, such as ours, e.g. CO_2^-, g-values of the g-tensor are close to the free spin value (g_e=2.0023), reflecting negligible orbital contribution to the magnetic moment of the molecule. The anisotropy of g-values depends on the symmetry of the paramagnetic molecule as well as on the near environment in which the molecule was embedded. The nuclear spin (I) couples with the unpaired electron forming a $2I+1$ lines of the spectra, viz. hyperfine structure, centered at g_o and spaced by the distance between the spectral to lines quantified by the hyperfine splitting tensor A. Values of the A tensor are larger in stronger couplings between the nuclear and electron spins. The parameters g or/and A, determine the type of paramagnetic ions and as well gives information on details of their structural environments. The EPR zero field splitting tensors D and E measure deviation of the ion crystal field from ideal tetrahedral or octahedral symmetries and apply only to the ions with more than one unpaired electrons, such as Mn^{2+} or Fe^3. In disordered lattices only D value can be obtained.

1. Lund, A., Shiotani, M., Shimada, S.: Principles and Applications of ESR Spectroscopy DOI: 10.1007/978-1-4020-5344-3, Springer (2011), ISBN: 978-1-4020-5344-6.

SI 2 Solubility boundaries calculations

Thermodynamic solubility product (thermodynamic equilibrium constant of dissolution) is expressed as a product of ionic activities (of constituent ions) in equilibrium. Thus, amorphous calcium carbonate, $CaCO_3 \cdot n\ H_2O$, (ACC), dissociate according to the equation:

$CaCO_3 \cdot n\ H_2O \leftrightarrow Ca^{2+} + CO_3^{2-}$,

solubility product is defined as:

$$K_{sp}^{o} = (a(Ca^{2+}) \cdot a(CO_3^{2-}))_{eq} = ((c(Ca^{2+})\ \gamma(Ca^{2+}) / c^{o}) \cdot (c(CO_3^{2-})\ \gamma(CO_3^{2-}) / c^{o}))_{eq}$$

Amorphous calcium phosphate, $Ca_3(PO_4)_2$, (ACP), dissociate according to the equation:

$Ca_3(PO_4)_2 \leftrightarrow 3Ca^{2+} + 2PO_4^{3-}$,

solubility product is defined as:

$$K_{sp}^{o} = (a(Ca^{2+})^3 \cdot a(PO_4^{3-})^2)_{eq} = ((c(Ca^{2+}) \cdot \gamma(Ca^{2+}) / c^{o})^3 \cdot (c(PO_4^{3-}) \cdot \gamma(PO_4^{3-}) / c^{o})^2)_{eq.}$$

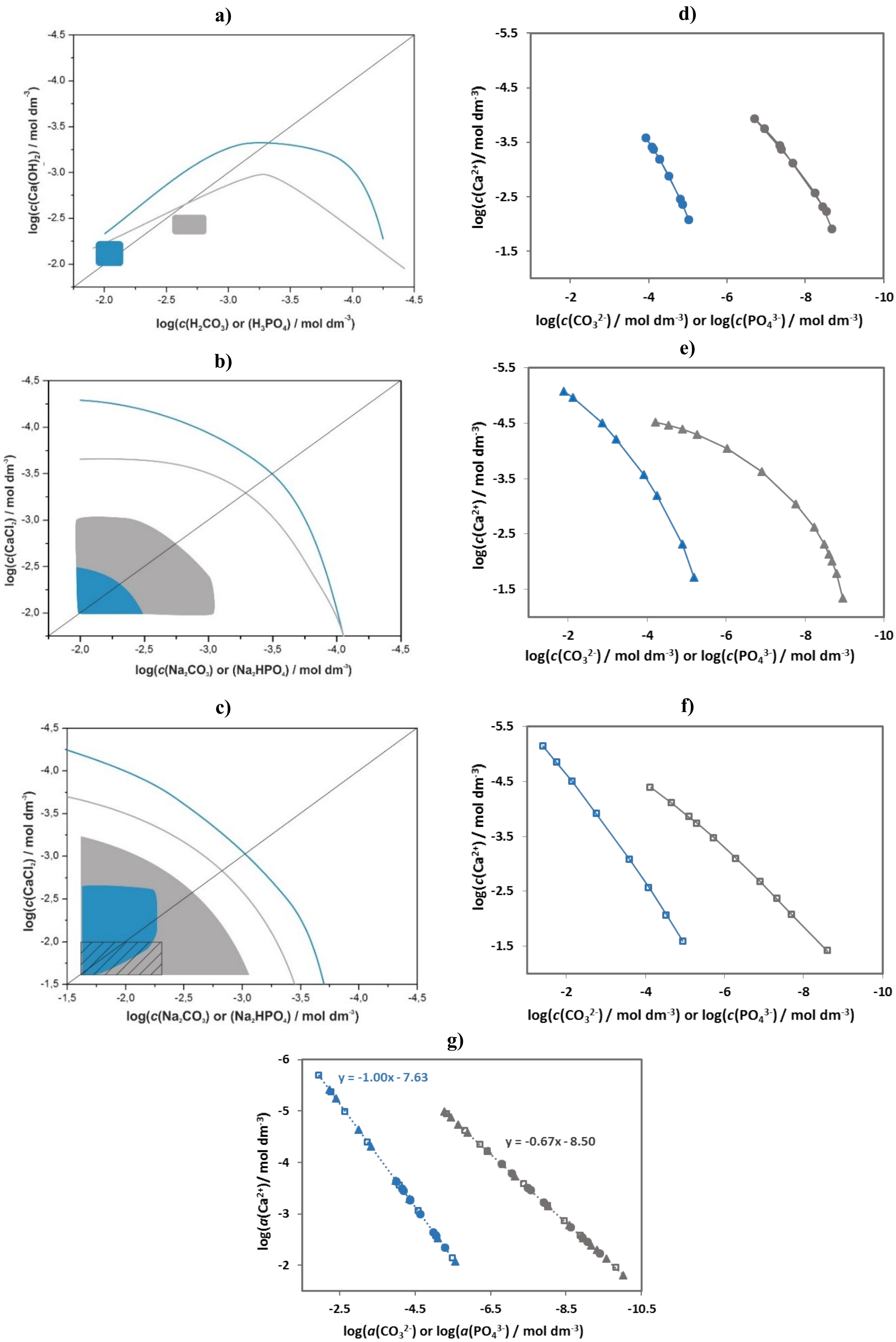

Figure SI 2. Precipitation diagrams in which supersaturations are shown as a function of total reactant concentrations (a-c) and corresponding plots in which the concentrations of constituent ions (d-f) or their activities (g) are used. A linear dependences in the activity plot, with the slopes of -1 and -2/3 for ACC and ACP, corresponds to the stoichiometry of different amorphous phases. Blue colour refers to ACC, while grey to ACP.

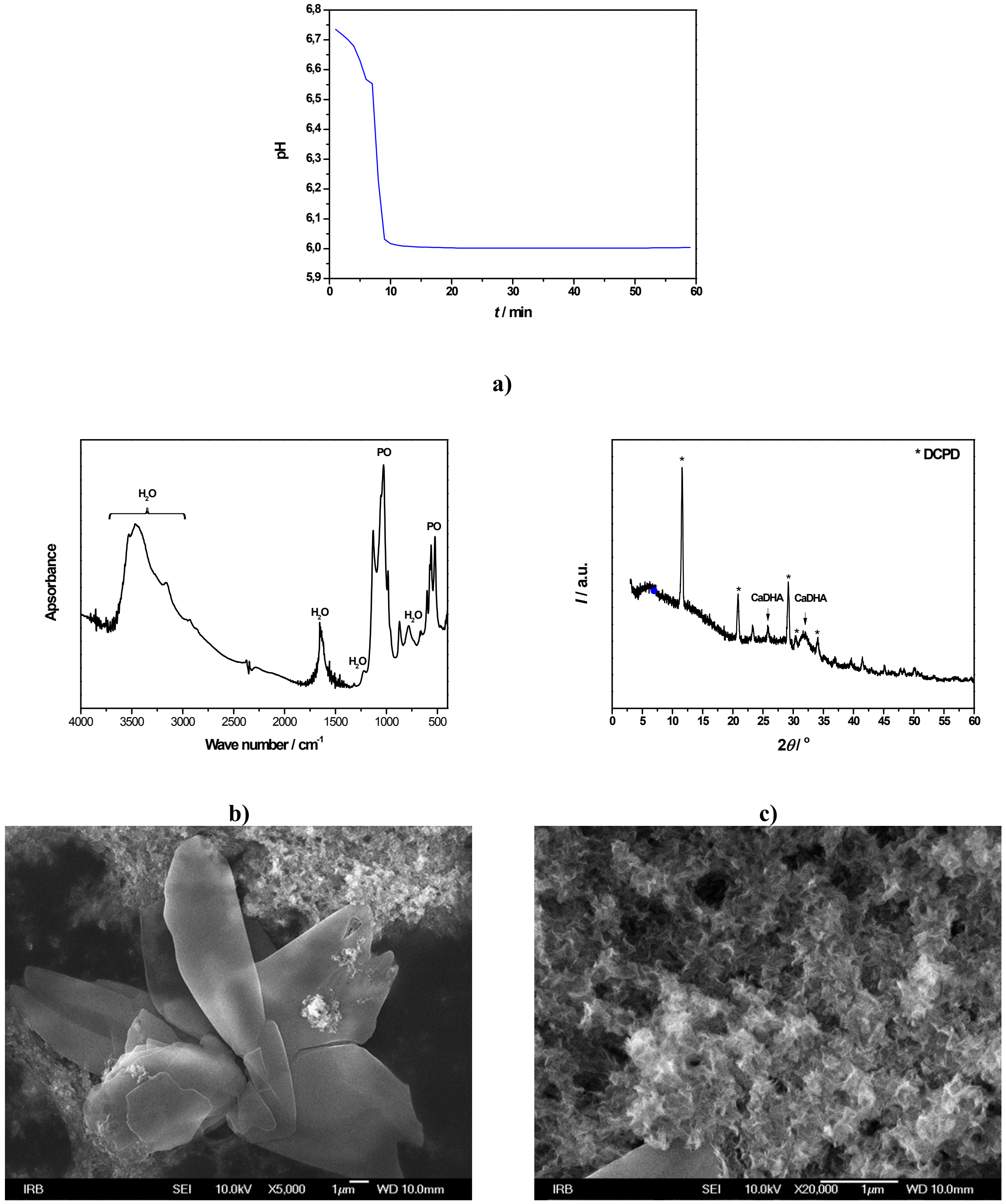

a)

b)

c)

d)

e)

Figure SI 3. a) pH curve, b) FTIR spectra, c) XRD diffractogram, d) and e) SEM micrograph of the mixture of DCPD and CaDHA formed in complex precipitation system at highest investigated reactant concentrations ($c(CaCl_2)$ = 0,01 mol dm^{-3}, $c(Na_2HPO_4)$ = 0,005 mol dm^{-3}) after 5 minutes aging time at 25 °C.

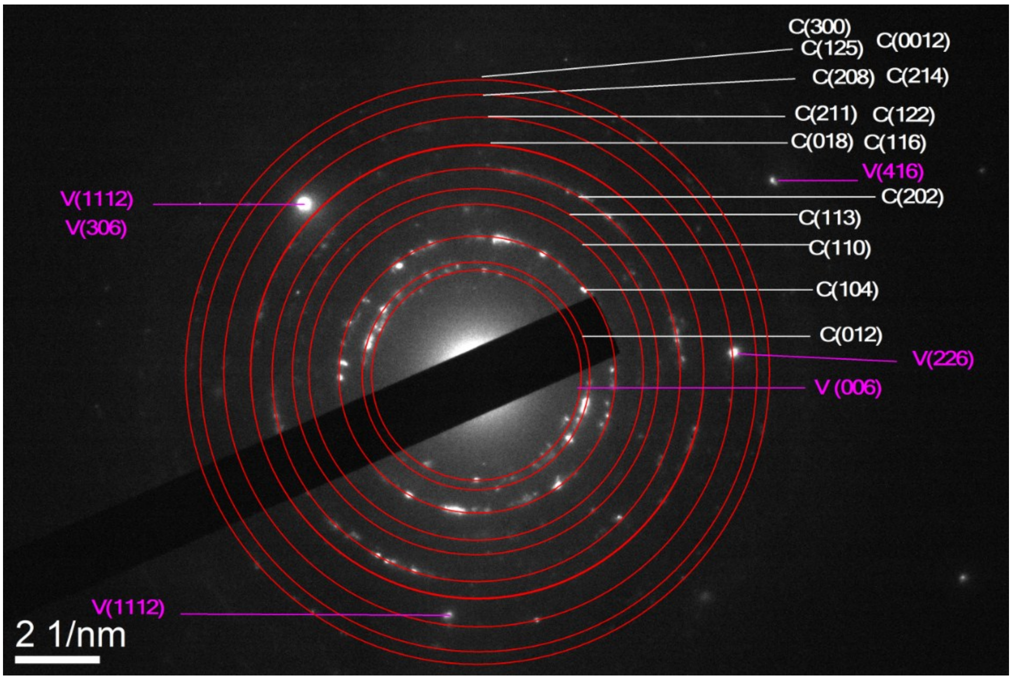

Figure SI 4. Enlarged SAED pattern of ACC$_{simple}$ showing partially crystallized to dominant calcite phase with presence of small amount vaterite phase.

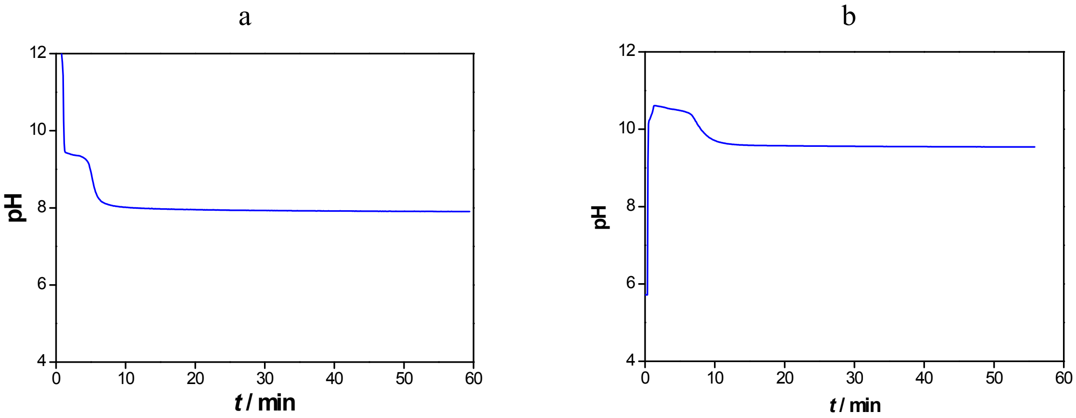

Figure SI 5. pH curves of the samples formed in CaCO$_3$ a) simple and b) complex system.

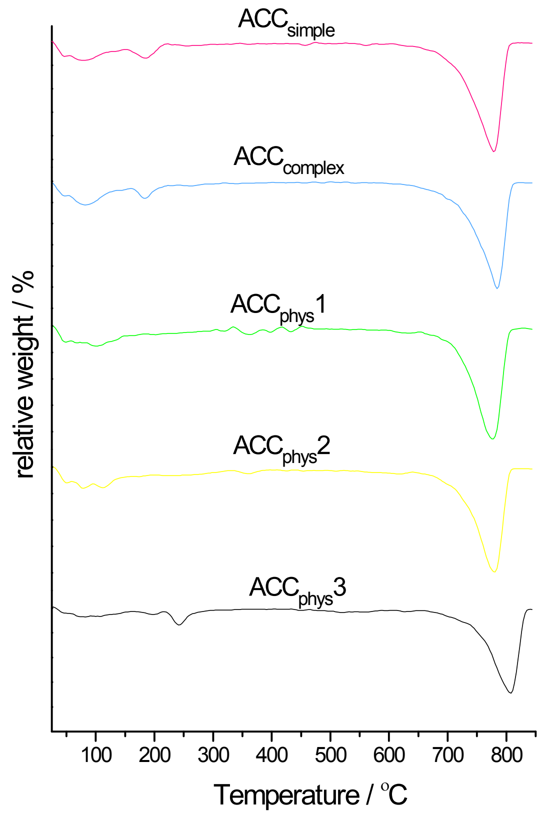

Figure SI 6. Comparative presentation of TGA results for amorphous precursors formed in $CaCO_3$ simple, complex and physiological systems.

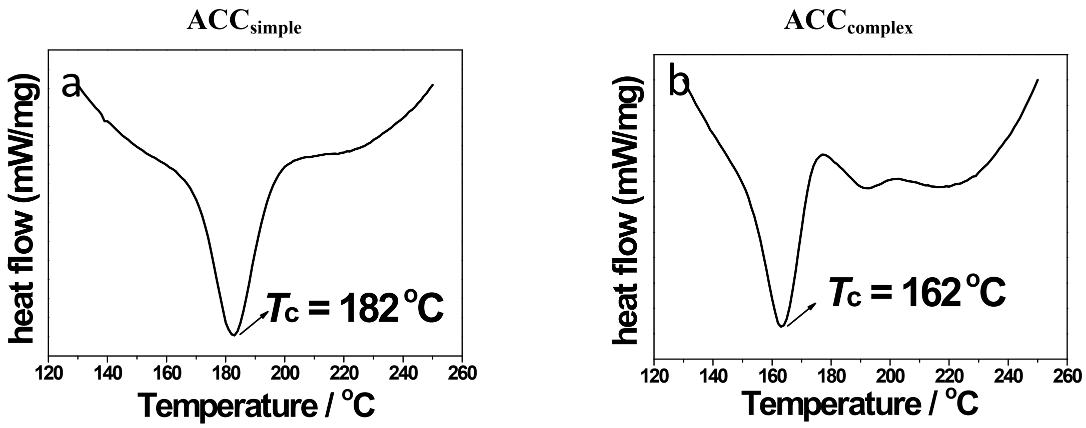

Figure SI 7. Enlarged DSC curves (insets in Figure 3e and j presented in the manuscript) for ACC_{simple} (a) and $ACC_{complex}$ (b), scale is determined according to the temperature of crystallization.

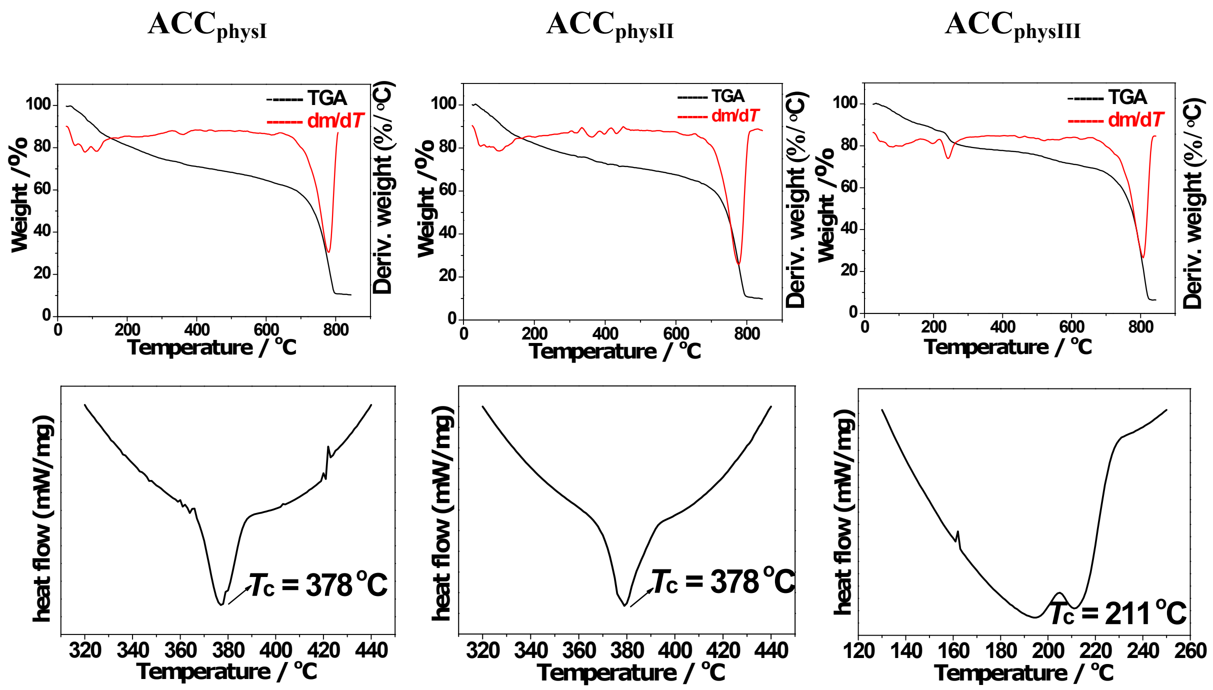

Figure SI 8. Enlarged TGA results (a, c and e) and DSC curves (b, d and f) for ACC_{physI}, ACC_{physII} (b) and $ACC_{physIII}$ (c)

ACP$_{\text{physI}}$

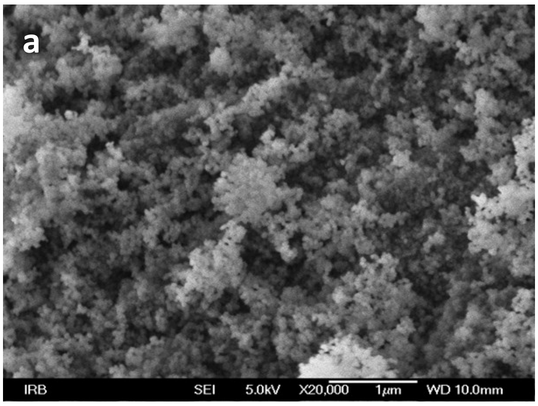

ACP$_{\text{physII}}$

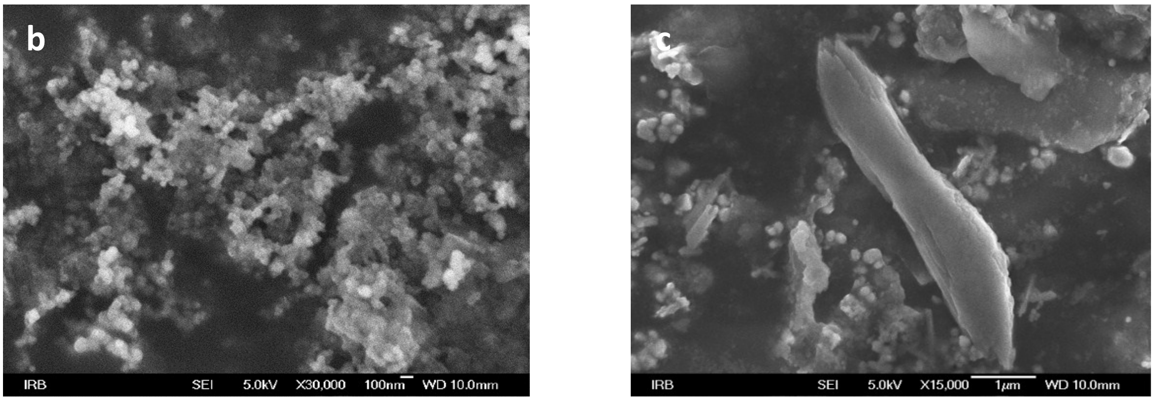

Figure SI 9. SEM micrographs of the precipitate obtained in physiological precipitation system at a) medium supersaturation ($c(\text{CaCl}_2) = 0.005$ mol dm^{-3}, $c(\text{Na}_2\text{HPO}_4) = 0.002$ mol dm^{-3}, $c(\text{MgCl}_2) = 0.01$ mol dm^{-3}, a-d, ACP$_{\text{physI}}$) and b)- c) high supersaturation ($c(\text{CaCl}_2) = c(\text{Na}_2\text{HPO}_4) = 0.01$ mol dm^{-3}, $c(\text{MgCl}_2) = 0.02$ mol dm^{-3}, ACP$_{\text{physII}}$) after 10 minutes aging time at 25 $^{\text{o}}$C. Scale bars: a) and c) 1 μm, b) 100 nm.

Figure SI 10. Selected area electron diffraction obtained from the plate-like crsytals (Fig. 5 i) formed in physiological precipitation system at high supersaturation ($c(CaCl_2) = c(Na_2HPO_4) = 0.01$ mol dm^{-3}, $c(MgCl_2) = 0.02$ mol dm^{-3}, e-h, ACP$_{physII}$) after 10 minutes aging time at 25 °C.

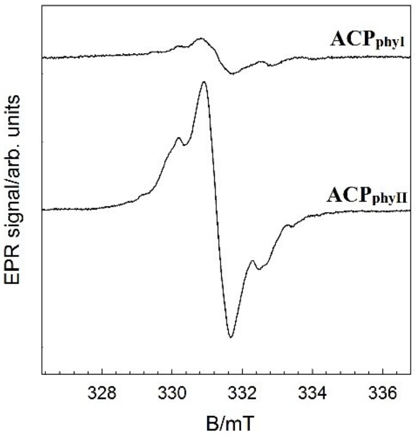

Figure SI 11. EPR spectra of γ-irradiated ACP precipitate formed in physiological system ACP_{physI} and ACP_{physII} after 10 minutes aging time.

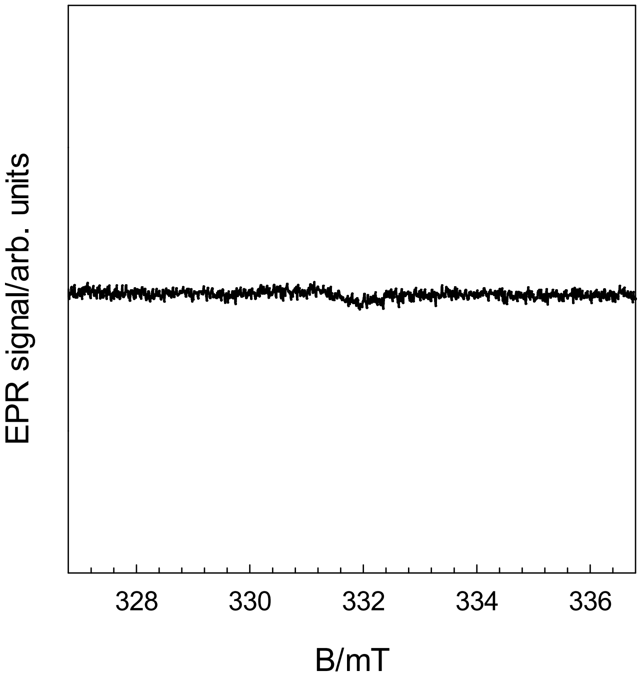

Figure SI 12. EPR spectra of γ-irradiated ACP precipitate formed in simple (ACP_{simple}) system for which in addition to the synthesis, isolation, irradiation and characterization was performed in the N_2 atmosphere.